J Neurophysiol 94: 1789–1797, 2005.
First published May 11, 2005; doi:10.1152/jn.00826.2004.

Spatial Distribution of Suppressive Signals Outside the Classical Receptive Field in Lateral Geniculate Nucleus

Ben S. Webb, Christopher J. Tinsley, Christopher J. Vincent, and Andrew M. Derrington
School of Psychology, University of Nottingham, Nottingham, United Kingdom

Submitted 12 August 2004; accepted in final form 10 May 2005

Webb, Ben S., Christopher J. Tinsley, Christopher J. Vincent, and Andrew M. Derrington. Spatial distribution of suppressive signals outside the classical receptive field in lateral geniculate nucleus. *J Neurophysiol* 94: 1789–1797, 2005. First published May 11, 2005; doi:10.1152/jn.00826.2004. A suppressive surround modulates the responsiveness of cells in the lateral geniculate nucleus (LGN), but we know nothing of its spatial structure or the way in which it combines signals arising from different locations. It is generally assumed that suppressive signals are either uniformly distributed or balanced in opposing regions outside the receptive field. Here, we examine the spatial distribution and summation of suppressive signals outside the receptive field in extracellular recordings from 46 LGN cells in anesthetized marmosets. The receptive field of each cell was stimulated with a drifting sinusoidal grating of the preferred size and spatial and temporal frequency; we probed different positions in the suppressive surround with either a large half-annular grating or a small circular grating patch of the preferred spatial and temporal frequency. In many of the cells with a strong suppressive surround (29/46), the spatial distribution of suppression showed clear deviation from circular symmetry. In the majority of these of cells, suppressive signals were spatially asymmetrical or balanced in opposing areas outside the receptive field. A suppressive area was larger than the classical receptive field itself and spatial summation within and between these areas was nonlinear. There was no bias for suppression to arise from foveal or nasal retina where cone density is higher and no other sign of a systematic spatial organization to the suppressive surround. We conclude that nonclassical suppressive signals in LGN deviate from circular symmetry and are nonlinearly combined.

INTRODUCTION

Like retinal ganglion cells, the classical receptive field of an lateral geniculate nucleus (LGN) cell is concentrically organized with antagonistic center and surround. Extending beyond the classical receptive-field of an LGN cell is a "suppressive field" (Hubel and Wiesel 1961; Levick et al. 2002; Singer and Creutzfeldt 1970). Stimulating the suppressive field—or the "extraclassical" or "nonclassical" surround—does not elicit a response but can modulate responses to stimuli on the classical receptive-field (Allman et al. 1985; Felisberti and Derrington 2001a,b; Marrocco and McClurkin 1985; McClurkin and Marrocco 1984; Sillito et al. 1993; Solomon et al. 2002; Webb et al. 2002).

Although we know much about the selectivity and mode of action of signals in the suppressive surround (Cleland et al. 1983; Cudeiro and Sillito 1996; Felisberti and Derrington 2001a,b; Jones and Sillito 1991; Jones et al. 2000; Marrocco and McClurkin 1985; Marrocco et al. 1982; Molotchnikoff and Cérat 1992; Murphy and Sillito 1987; Rivadulla et al. 2002; Sillito et al. 1993; Solomon et al. 2002; Vidyasagar and Urbas 1982; Webb et al. 2002), we know nothing about their spatial distribution. An untested assumption is that suppressive signals are distributed uniformly or balanced in opposing regions outside the receptive field. However, stimulating an area encircling the receptive field or areas on opposite sides of the receptive field may mask suppressive signals arising from localized zones, or "hot spots." For example, the suppression generated by stimulating a uniform area encircling the receptive field may arise exclusively from a smaller, discrete location.

We know that suppressive signals arise nonuniformly outside V1 receptive fields. Walker et al. (1999) examined the spatial distribution of suppression in cat V1. When they probed different positions outside the receptive field with a grating of the same spatial dimensions as the receptive field, they found that in most cells, suppressive signals arose from a small, discrete, "asymmetrical" region. Except for a slight tendency for greater suppression from the ends of the receptive field, they found little evidence of any systematic organization to suppressive zones outside the receptive fields of V1 cells (Walker et al. 1999). In macaque V1 cells, suppression can also arise asymmetrically (Cavanaugh et al. 2002b; Jones et al. 2001) and is often strongest when the ends of the receptive field are stimulated with a grating of the preferred orientation or the sides of the receptive field are stimulated with a grating of an orthogonal orientation (Cavanaugh et al. 2002b). In marmoset V1, we found that suppression strength was uncorrelated on the ends and sides of the receptive field, suggesting that it may arise nonuniformly (Webb et al. 2003).

The aim of the experiments described here is to characterize the spatial distribution of suppressive signals outside the receptive field of primate LGN cells. Walker et al. (1999) examined the distribution of suppressive signals outside the receptive field of five cat LGN cells. In one of these cells, suppression arose from a single, discrete zone outside the receptive field. The distribution of suppressive signals in LGN could take several different forms, however, arising either uniformly from an area that encircles the receptive field, symmetrically along the same axis or nonuniformly from large or small single or multiple discrete zones outside the receptive field. Here, we consider each of these possibilities by examining the fine and coarse spatial distribution and linearity of summation of suppressive signals outside the receptive field of LGN cells in anesthetized marmosets.

Address for reprint requests and other correspondence: B. Webb, School of Psychology, University of Nottingham, University Park, Nottingham NG7 2RD, UK (E-mail: bsw@psychology.nottingham.ac.uk).

The costs of publication of this article were defrayed in part by the payment of page charges. The article must therefore be hereby marked "*advertisement*" in accordance with 18 U.S.C. Section 1734 solely to indicate this fact.

METHODS

Electrophysiology

We recorded extracellular responses in the LGN of three anesthetized, paralyzed marmosets (*Callithrix jacchus*). We have described the methods used in our laboratory before (Webb et al. 2002). Here, we provide a brief overview. An experiment typically lasted 5 days, during which a constant level of anesthesia and paralysis were maintained with fentanyl citrate (20 $\mu g \cdot kg^{-1} \cdot h^{-1}$) and vecuronium bromide (0.1 $mg \cdot kg^{-1} \cdot h^{-1}$). The animal was artificially respired with a mixture of N_2O (70%) and O_2 (30%), and body temperature was maintained at 37.5°C. Electrocardio- and electroencephalogram activity were monitored throughout the experiment. The eyes were protected with gas-permeable lenses; their refractive error was corrected with miniature spectacle lenses that maximized the response of the first cell to a high spatial-frequency grating. Analogue signals from epoxy-coated electrodes advanced into the LGN were sent to an amplifier, band-pass filtered and time-stamped with a resolution of 100 μs. We constructed a template of putative spikes by averaging multiple traces; spikes were matched to this template using a goodness-of-fit criterion.

Visual stimuli

We generated achromatic stimuli with a Macintosh computer using a Radius 10-bit graphics card. We mapped receptive fields initially on a tangent projection screen. A horizontally oriented, full-field, drifting sinusoidal grating of 100% contrast was presented on the tangent screen while searching for cells. Once we encountered a cell. its spiking activity was isolated, ocular dominance was determined and the nonpreferred eye covered. Its receptive field was mapped on the tangent screen with a small (typically, 1° diam) patch of drifting sinusoidal grating optimized in spatial and temporal frequency to elicit the largest response. We then transferred the receptive field to the center of a CRT display. We re-mapped receptive fields on the CRT display with the smallest patch of drifting grating that elicited a reliable response (typically, 0.2–0.5° diam). An LGN cell's polarity (on or off center) was determined by comparing its response to flashed bright and dark spots. We measured the size of the classical receptive-field center with flashed spots of different diameters. In order, we obtained steady-state measurements of spatial frequency, temporal frequency, and size tuning in separate tests by varying a drifting grating along each of these dimensions in equal logarithmic steps. We also estimated receptive-field size by varying the inner diameter of an annular grating. In three cells, this estimate was larger than that obtained with grating patches. In these cases, we defined receptive-field size as the smallest inner diameter of an annular grating of the preferred spatial and temporal frequency that elicited no response. Otherwise, we defined receptive-field size as the smallest grating patch diameter of the preferred spatial and temporal frequency that elicited the largest response. At any sign that stimuli were not centered on the receptive field, we re-mapped the receptive field as described in the preceding text. Finally, we measured responses of each cell to an optimal patch of drifting grating whose contrast ranged in equal logarithmic steps between 0.016 and 1. For experimental tests, contrast of the grating on the receptive field was set to evoke responses within the dynamic range of the cell.

We examined the fine and coarse spatial organization of suppressive zones outside the receptive field in separate experiments. Both experiments had the same general design. The receptive field was stimulated with a circular patch of drifting grating presented alone or in conjunction with a contiguous grating of 100% contrast outside the receptive-field. Each configuration outside the receptive field was presented alone to ensure that it did not cause a response. All of the stimuli used here were presented at a horizontal orientation and at the preferred spatial and temporal frequencies. We consider responses to the grating on the receptive field as a baseline measurement, below which responses are reduced due to the presence of a stimulus outside the receptive field. We never observed an increase above this baseline with any stimulus configuration.

The coarse organization of the suppressive surround was probed with a half-annular grating presented at four overlapping locations, above, below, and on either side of the receptive field. An annular grating—the sum of two half-annular gratings—was included as a control stimulus; its outer diameter was three times that of the grating on the receptive-field (see Fig. 1*A*).

We also considered that suppression may arise from discrete pockets, or hot spots, outside the receptive field (Walker et al. 1999). In a subset of our sample, a circular grating patch was presented at eight overlapping locations within an annular region. The diameter of this grating patch was the same as that on the receptive field. Its position outside the receptive-field is defined by a vector originating at the center of the receptive field with a magnitude equal to the diameter of the receptive field and a 45° angular separation from its neighbor. A grating presented at any of the eight locations outside the receptive field was therefore equidistant from the center of the receptive field. In this experiment, we used an annular grating that covered the area tiled by the grating patches outside the receptive field. Note that the diameter of this annular grating is also three times that of the grating on the receptive field (see Fig. 1*B*).

In both experiments, stimuli were randomly interleaved within a block, which included a blank screen of mean luminance to measure the spontaneous rate; each block of stimuli was repeated 10 times. A stimulus was presented for 1 s with an interstimulus interval of 0.5 s.

Quantification of a- and bisymmetrical suppression

To quantify the spatial distribution of suppressive signals outside the receptive field, we used a circular statistic metric (Batschelet 1981) that has been used before in research on the spatial organization of the receptive-field surround in the middle temporal area (Xiao 1995) and in V1 (Cavanaugh et al. 2002b; Jones et al. 2001; Walker

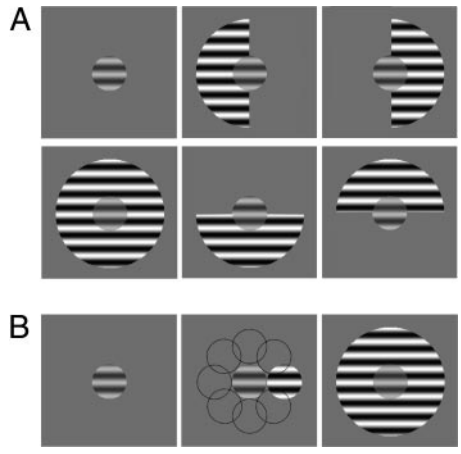

FIG. 1. Schematic illustration of stimuli used to examine the spatial distribution of suppressive signals outside the classical receptive field in lateral geniculate nucleus (LGN). In both experiments, the classical receptive field was stimulated with a drifting luminance-modulated sinusoidal grating of the preferred diameter, spatial and temporal frequency, and a contrast that did not saturate a cell's response. *A*: coarse organization of suppressive signals outside the receptive field was probed with a half-annular grating presented above, below, and on either side of the receptive field. An annular grating—the sum of 2 half-annular gratings—of 3 times the diameter of the grating on the receptive field was included in the stimulus set as a control. *B*: fine organization outside the receptive field was probed with a grating patch of the same dimensions as the grating on the receptive field, presented at 8 overlapping locations equidistant from the center of the receptive field. The dashed circles indicate each of these locations which tile the area inside the control annulus shown on the right.

et al. 1999). First, we calculated the magnitude of suppression at each position outside the receptive-field: $S_i = R_c - R_{ec}/R_c$, where R_c is the response to the grating on the receptive field and R_{ec} is the response to the grating on the receptive field in the presence of a grating at a given position outside the receptive field. In the experiment with half-annular gratings, S_i is the magnitude of suppression at four locations ($i = 1–4$) outside the receptive field; in the experiment with small grating patches, S_i is the magnitude of suppression at eight locations ($i = 1–8$).

We then calculated a suppression index (SI) for each cell

$$SI_1 = \frac{\sqrt{(\sum_i^n S_i \times \sin(\alpha_i))^2 + (\sum_i^n S_i \times \cos(\alpha_i))^2}}{\sum_i^n S_i} \quad (1)$$

This equation quantifies the magnitude of suppression (S_i) arising from a given position (α_i) outside the receptive field. Pointing to each position outside the receptive field is a vector the length of which represents the magnitude of suppression arising from that position. The magnitude of the vector, SI_1, is the sum of all the vectors pointing to each position, normalized by their total length. SI_1 approaches 0 if suppression arising from each position outside the receptive field has the same magnitude and approaches 1 when suppression arises exclusively from a single position.

If suppression is not circularly symmetrical but is distributed symmetrically along a single axis, SI_1 values will be close to zero. Therefore a second index, SI_2, was calculated to quantify the strength of suppression on different axes. *Equation 1* was used to calculate SI_2, but the angle of each position outside the receptive-field (α_i) was doubled. The consequence is that SI_2 has a value of 1 if suppression arises on a single axis and a value of 0 if suppression on different axes has the same magnitude. For example, if suppression was balanced on opposite sides of the receptive-field SI_2 will equal 1.

Equation 1 returns the length of the suppression index vector but not its angle. To quantify the angle of the suppression index vector, we used the following equation

$$\text{ang}(SI) = \arctan\left(\frac{\sum_i^n S_i \times \sin(\alpha_i)}{\sum_i^n S_i \times \cos(\alpha_i)}\right) \quad (2)$$

For the SI_1 vector, ang(SI) indicates the position outside the receptive field where most suppression arises. For the SI_2 vector, ang(SI) indicates the axis along which most suppression arises.

RESULTS

We examined the spatial distribution of suppressive signals outside the receptive field of 30 parvocellular (P) cells and 16 magnocellular (M) cells, of which 25 were on center and 21 were off center cells, the receptive fields of which were between 1 and 36° from the fovea. Responses are expressed as the amplitude of the Fourier component of the discharge rate at the temporal frequency of stimulation. One cell was excluded from further analysis because it did not respond to any stimulus used here at >2 SDs above the mean spontaneous rate.

Spatial form of suppression

Signals from outside an LGN cell's receptive-field typically reduce its response (Solomon et al. 2002; Webb et al. 2002). The spatial distribution of such suppressive signals could take several different forms, arising either uniformly from an area that surrounds the receptive field, symmetrically along one axis, or nonuniformly from single or multiple discrete zones outside the receptive field. We begin by showing responses of a representative cell in our sample in which the spatial distribution of suppression outside the classical receptive field shows clear deviation from circular symmetry.

Figure 2*A* shows responses of an off center P cell to a small patch of drifting grating. This response was reduced from 51 ± 2.28 to 24 ±1.59 (SE) imp/s by the presence of an annular grating surrounding the receptive field (Fig. 2*B*). When the annular grating was presented alone, it reduced the spontaneous rate from 4.1 ± 0.68 (Fig. 2*C*) to 2 ± 0.62 imp/s (modulation amplitude: 2.7 ± 0.71 spike/s; Fig. 2*D*) but not enough to account for the reduction in evoked activity. Stimulating the suppressive surround with a half-annular grating above the receptive field also substantially reduced responses, to 28 ± 1.88 imp/s (Fig. 2*B*), whereas below, right, and left of the receptive field, it caused negligible suppression, reducing responses to 42 ± 1.49 (Fig. 2*F*), 42 ± 2.72 (Fig. 2*G*), and 49 ± 2.2 imp/s (Fig. 2*H*), respectively. Thus in this cell, most suppression arose from an area above the receptive field. Stimulating a larger area encircling the receptive field added very little to the magnitude of suppression, suggesting that suppressive signals do not arise uniformly outside the receptive field and are nonlinearly combined.

In many of the cells (13) with a strong suppressive surround (29; see following text), suppression arose asymmetrically from a relatively large area. Figure 3 shows responses of three such cells (Fig. 3*C* is the cell shown in Fig. 2). Each column shows responses of a single cell to an optimal grating on the receptive field when four positions outside the receptive field were probed with a half-annular grating (*top*) and eight positions were probed with a small circular grating patch (*bottom*). Responses are presented in polar plots in which grating position outside the receptive field is represented by polar angle, and response amplitude (imp/s) is represented by radial dis-

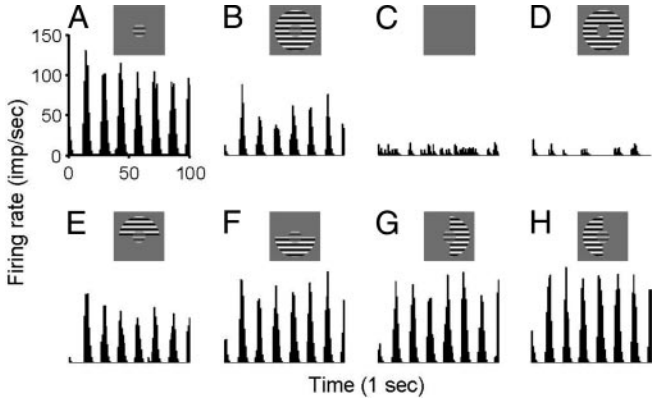

FIG. 2. Example of asymmetrical suppression in a parvocellular (P) off center cell. Stimulating the suppressive surround with a half-annular grating above the receptive field (*E*) reduced responses to the grating on the receptive field (*A*, diameter, 3°; contrast, 75%) by almost the same degree as an annular grating (*B*), whereas a half-annular grating presented below (*F*), right (*G*), and left (*H*) of the receptive field caused negligible suppression. The annular grating presented alone did not elicit a response (compare *D* and *C*), demonstrating that it had not encroached onto the receptive field. Suppressive surround grating contrast, 100%; spatial frequency, 0.5 cycles/°; temporal frequency, 8 cycles/s; 10-ms bins.

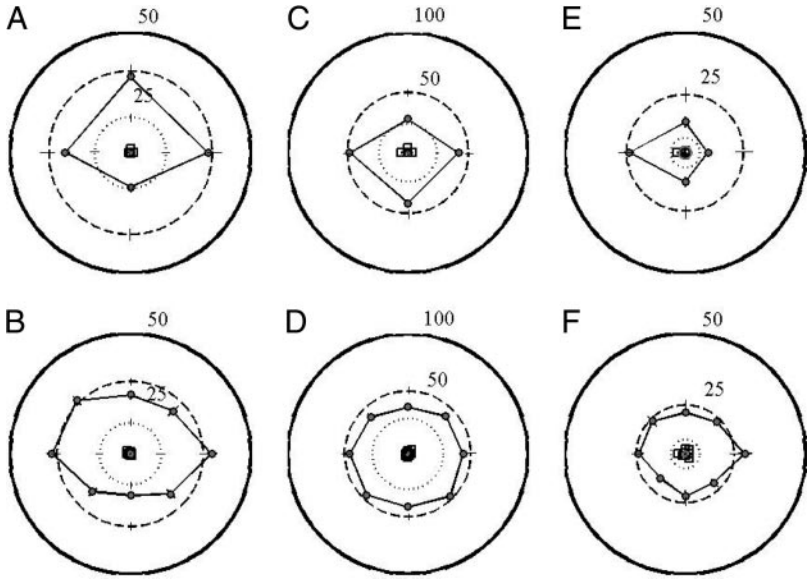

FIG. 3. Examples of asymmetrical suppression in 3 LGN neurons. *Top*: from left to right, responses of 2 P cells and an magnocellular (M) cell to a grating on the receptive field, presented alone or in conjunction with a half-annular grating, presented at four overlapping positions in the suppressive surround. *Bottom*: how responses of the same 3 neurons are modulated by circular grating patches presented at 8 overlapping positions in the suppressive surround. The radial axis represents response amplitude (imp/s) and angular position represents position of a stimulus beyond the receptive field. - - -, the mean response to a grating patch of intermediate contrast presented alone on the receptive field. · · · , the mean response to stimulation of the receptive field plus stimulation of the suppressive surround with an annular grating. ◍ — ◍ the mean response to stimulation of the receptive field plus 1 of the half-annular gratings (*top*) or 1 of the small grating patches (*bottom*) in the suppressive surround. □ — □ (near the origin in each plot), responses to gratings presented in the suppressive surround alone. These stimuli did not drive neurons, and therefore elicit responses near the mean spontaneous activity (▬). Radial error bars indicate ± SE. The SI_1 values for each panel are *A,* 0.59; *B,* 0.48; *C,* 0.38; *D,* 0.23; *E,* 0.35; *F,* 0.11.

tance from the origin. The - - - shows the response of each cell to the central grating patch alone. Data points that plot near this line indicate positions that evoked little suppression. The · · · shows the response to the combination of the central patch and a full-contrast annular grating. Data points that plot near this line indicate positions that contribute strongly to the suppressive signal. Figure 3*A* shows a cell that was most suppressed when a half-annular grating was presented in the quadrant below the receptive field. When the suppressive surround was stimulated with smaller circular grating patches (Fig. 3*B*), the most potent position was found to be directly under the receptive field. For the cell in Fig. 3, *C* and *D*, the region above the receptive field contributes most to the suppressive signal. In both these cases, small circular grating patches elicited weaker suppression than half-annular gratings. The same is not true for the cell depicted in Fig. 3, *E* and *F*; a half-annular grating on the right side of the receptive field elicited substantial suppression (Fig. 3*E*), whereas probing with a smaller grating patch within the same area failed to elicit any reduction in response (Fig. 3*F*). This was the only cell in which we found that probing within a large suppressive area with a smaller grating patch failed to elicit any suppression. In other cells, we always found that if a half-annular grating elicited suppression from outside the receptive field, presenting a smaller grating patch anywhere within the same half-annular region elicited weaker suppression. These observations suggest that suppressive signals arise from a large area that does not encircle the receptive field.

In a different set of cells (10), suppression was balanced in opposing regions outside the receptive field. Two examples of this form of suppression are shown in Fig. 4. Conventions and notation are the same as in Fig. 3. The *top row* shows two cells (Fig. 4, *A* and *C*) in which the areas above and below the receptive field contribute more to the suppressive signal than the areas on either side of the receptive field. This form of suppression, however, is weaker than that elicited by an annular grating surrounding the receptive field. The *bottom row* shows that probing within these suppressive areas with a smaller grating patch elicited similar levels of suppression from the ends of the receptive field in one of the cells (Fig. 4*D*) and weaker suppression along an oblique axis in the other (Fig. 4*B*).

In a small subset of our sample (6 cells), we also found that suppression arose uniformly from a region encircling the receptive field (data not shown here). In these cells, a half-annular grating elicited similar levels of suppression from each of the four positions outside the receptive field, which was typically weaker than that elicited by an annular grating. Probing with small grating patches elicited even weaker suppression, uniformly distributed around the receptive field.

The *SI* vectors (see METHODS) provide a useful means of quantifying the proportion of cells receiving different patterns of suppression from outside the receptive field but are meaningless when suppression is negligible. We only consider cells

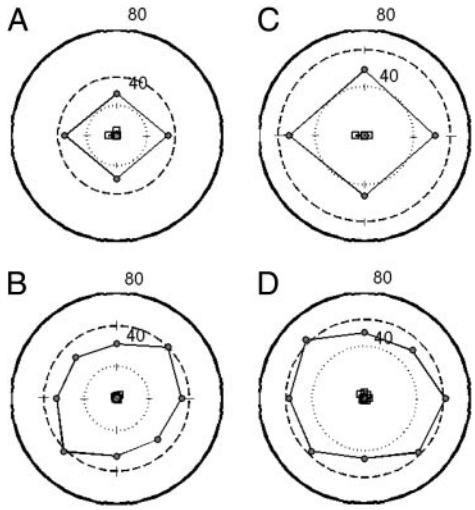

FIG. 4. Examples of bisymmetrical suppression in 2 LGN neurons. Notation is the same as in Fig. 3. *Top*: half-annular gratings presented at each end of the receptive field of 2 P cells reduce responses to almost the same extent as an annular grating in the suppressive surround. *B*: presenting small grating patches in the suppressive surround revealed that the bisymmetric suppression represented in *A* originates along an oblique axis. *D*: presenting small grating patches in the suppressive surround confirmed that the bisymmetric suppression represented in *C* originates from the ends of the receptive field. The SI_2 values for each panel are *A,* 0.41; *B,* 0.43; *C,* 0.29; *D,* 0.73.

whose responses were reduced by ≥20% when an annular grating was present outside the receptive-field (15 P cells, 14 M cells). Of the 17 cells that we excluded from further analysis, 15 were P cells, 2 were M cells, 7 were on center and 10 were off center cells. The much higher proportion of P cells with a weak suppressive surround is consistent with known properties of LGN cells (Solomon et al. 2002; Webb et al. 2002). Eight positions were probed outside the receptive field in 19 (9 P cells, 10 M cells)/29 cells with a strong suppressive surround. Our qualitative observations (see Figs. 3 and 4) suggest that different patterns of suppression (i.e., asymmetrical vs. bisymmetrical) may arise in different sets of cells. However, a statistical comparison of SI_1 and SI_2 values across these cells when we probed four positions outside the receptive field did not reveal a quantitative basis for such a categorization ($t = -1.45$, $P = 0.16$).

Size, selectivity, and summation outside the classical receptive field

We have established that in a subset of our sample, the spatial distribution of suppression outside the classical receptive field deviates from circular symmetry. Here we consider the size and selectivity of suppressive areas outside the classical receptive field and linearity of spatial summation within and between them. We found no statistical differences between P and M cells, so they are pooled in the following analyses. The examples in Figs. 3 and 4 suggest that a suppressive area outside the receptive field is considerably larger than the receptive field itself. If this is true then an appropriately positioned half-annular grating should elicit proportionally more suppression than a small circular grating patch. Alternatively, if a suppressive area is the same size as the receptive field, then an appropriately positioned small grating patch should elicit most of the suppressive signal. A further possibility is that suppression arises from multiple discrete areas or a uniform area encircling the receptive field, in which case an annulus would generate more suppression than any single grating patch or half-annulus.

To test these possibilities, we examined the normalized suppression (S_i; Fig. 5, *A–C*) and absolute suppression (imp/s; Fig. 5, *D* and *E*) generated by each stimulus class. The strength of suppression elicited by an annular grating is plotted against that elicited by the most-suppressive half-annular grating (Fig. 5*A*) and most-suppressive small grating patch (Fig. 5*B*). The dashed (Fig. 5*A*) and solid (Fig. 5*B*) gray diagonal lines in these plots are the linear prediction: the suppression generated by a half-annular grating or small grating patch is proportional to the area of the patch. The half-annular grating should produce half the suppression of an annular grating (Fig. 5*A*) and a small grating patch should generate one-eighth of that produced by an annular grating (Fig. 5*B*). In Fig. 5*A*, most of the data points fall between the solid and dashed diagonal lines, indicating that a half-annular grating generated weaker ($\mu = 0.33$; $\sigma = 0.1$) but not proportionally less suppression than an annular grating (0.44 ± 0.13). These means were statistically different ($t = 6.69$, $P = 2.92 \times 10^{-7}$). Most of the data points in Fig. 5*B* fall closer to the black diagonal than to the gray diagonal line, indicating that a small grating patch generated proportionally more suppression (0.25 ± 0.07) than a half-annular grating and proportionally more suppression than an annular grating (0.47 ± 0.13). These means were also statistically different ($t = -10.4$, $P = 4.83 \times 10^{-9}$). When one compares the strength of suppression generated by a half-annular grating with that generated by a small grating patch (Fig. 5*C*), it is clear that in most cells a half-annular grating generates stronger suppression ($t = -6.36$, $P = 5.4 \times 10^{-6}$). For neurons with low response rates, certain stimuli might generate a very high S_i because of a few additional spikes to that stimulus. To evaluate the absolute magnitude of suppression generated by each stimulus, in Fig. 5, *D–F,* we show the same comparisons as in Fig. 5, *A–C,* for absolute suppression of spike rate. Absolute suppression operates over a broad range of spike rates with the same pattern for each stimulus as that obtained for normalized suppression. These observations strongly suggest that, for most cells in our sample with a strong suppressive surround, suppressive signals arise predominantly but not exclusively from a large area outside the receptive field, which is not circularly symmetrical.

There is a potential caveat with this conclusion. Although the spatial-frequency of half-annular gratings used here is beyond that which can be resolved by the classical surround,

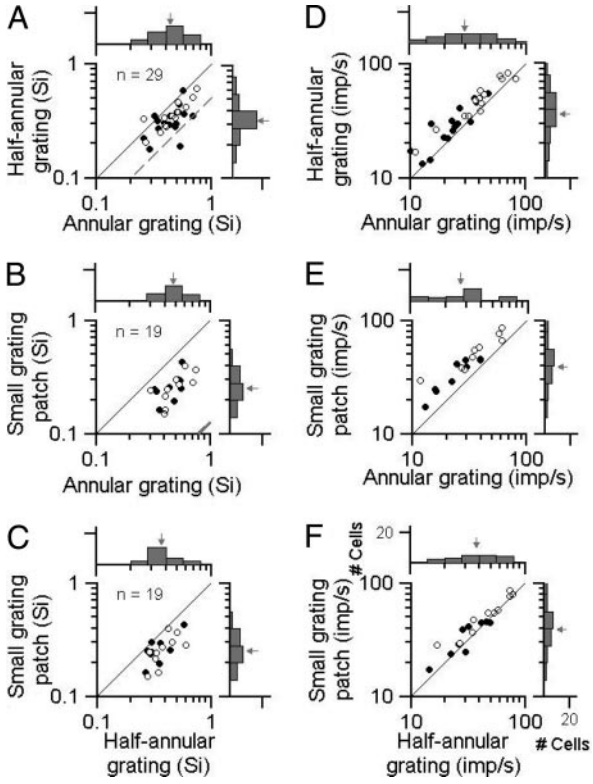

FIG. 5. Size and selectivity of suppressive areas outside the receptive field. The suppression generated for each neuron by the presence of an annular grating outside the receptive field is plotted against that generated by the most-suppressive half-annular grating (*A*) and most-suppressive small grating patch (*B*). The diagonal dashed and solid gray lines are the linear predictions that the strength of suppression generated by the most-suppressive half-annular grating (*A*) and small grating patch (*B*) is scaled proportionally (i.e., scaled by one-half and one-eighth, respectively). *C*: the suppression generated by the most-suppressive half-annular grating compared with that generated by the most-suppressive small grating patch. *D–F*: the same comparisons as in *A–C* for absolute response amplitude (imp/s). Distributions of the suppression index and response amplitude for each stimulus are presented in marginal histograms. The vertical arrows indicate the geometric mean of each distribution. Suppression values were calculated from *Eq. 6*-1. ● and ○, P and M cells, respectively.

blurring by the optic media will increase energy (at a range of frequencies) at the inner of edge of such high contrast stimuli. If these aberrant frequencies activated the classical surround, then even a mild anisotropy in the receptive field could produce the results we report here. This potential confound would be particular salient in M cells with their high contrast sensitivity. This seems an unlikely explanation for our results, however, because our control data clearly show that surround stimuli very rarely caused any response modulation in either M or P cells. When it was present (in 3 P cells and 1 M cell), it was of similar amplitude for each of the half-annular gratings and always less than spontaneous activity.

One question not considered in the preceding text is whether suppressive signals outside the classical receptive field are linearly combined. If they are linearly summed, then the sum of suppression generated by two opposing half-annular gratings should be equivalent to the suppression generated by an annular grating. We examine this possibility in Fig. 6. For each cell, we plot the sum of suppression generated by opposing half-annular gratings on the axes of minimal (Fig. 6*A*) and maximal suppression (Fig. 6*B*) against the suppression generated by an annular grating. The lack of clustering on the unity line in Fig. 6, *A* and *B,* indicates that suppressive signals are not combined linearly. If one assumes there is either a single dominant "warm area" or a warm area at each end of the maximum suppression axis, then summation along the minimum suppression axis reflects summation within one or two subunits, whereas summation along the maximum suppression axis represents either summation between one subunit and nothing or summation between two subunits. Figure 6*A* shows that summation within the suppressive subunits on the minimal suppression axis is super-linear (most data points fall below the line). This is just what would be expected if there were a threshold or some other type of positively accelerating nonlinearity in the receptive fields of the neurons that sum the visual signals that generate the suppression. Positively accelerating nonlinearities are common in marmoset LGN receptive fields (Felisberti and Derrington 2001a; Kremers et al. 2001; Solomon et al. 2002; Webb et al. 2002). On the other hand, Fig. 7*B* shows that summation between the suppressive subunits on the maximum suppression axis is sublinear (most data points fall above the line). This indicates that the summation between inhibitory subunits is a different process from the summation within subunits and presumably takes place at a different synapse. This difference is further emphasized by Fig. 6*C,* which shows that the sum of the separate suppressive effects at each end of the maximum suppression axis (which reflects the result of summation within sub-units) is greater than the sum of the suppressive effects at opposite ends of the minimum summation axis (which reflects summation between subunits).

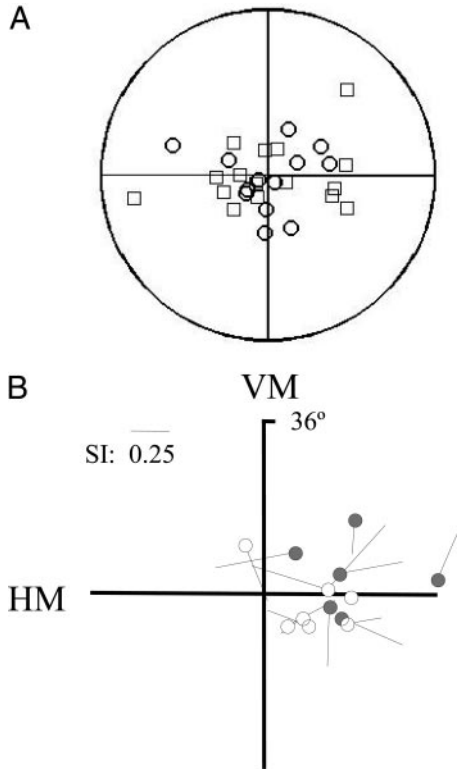

FIG. 7. Spatial location and eccentricity of suppressive zones. *A*: the coarse organization of suppressive zones outside the classical receptive field. Each data point represents the end of an *SI* vector from a single neuron. The origin represents an *SI* value of 0, and the outer edge of the plot represents an *SI* value of 1. The angular position of each point represents the location of a suppressive zone. ○ and □, SI_1 and SI_2 vectors, respectively. We have plotted only 1 direction of the *axis* represented by each SI_2 vector. *B*: the eccentricities of neurons in which suppression arose asymmetrically, when 4 locations were probed outside the receptive field. ◍, neurons receiving input from the contralateral eye; ○, neurons receiving input from the ipsilateral eye. The line emanating from each data point represents an SI_1 vector, pointing in the most suppressive direction; the length of each vector represents the magnitude of suppression. The axes are normalized to the largest eccentricity. HM, horizontal meridian; VM, vertical meridian.

Spatial distribution of suppressive areas

We asked if there was any systematic spatial organization to the location of suppressive areas outside the receptive field. This an important question because it may give a clue to the source of suppression. We address this question by examining

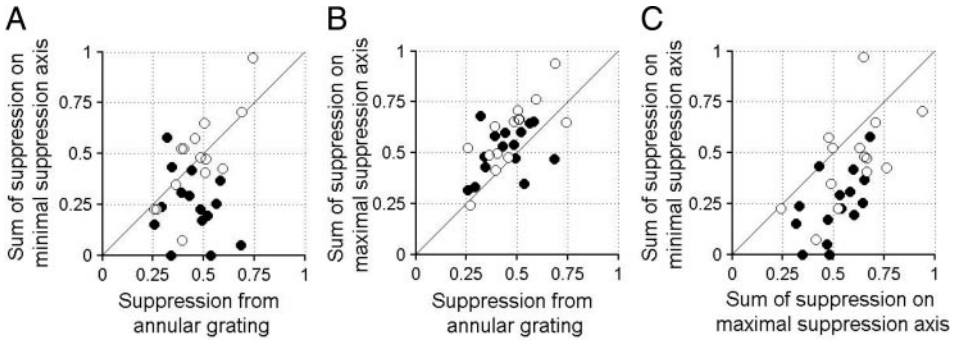

FIG. 6. Linearity of spatial summation outside the receptive field. *A* and *B*: the relationship between the sum of the suppression generated by half-annular gratings on the minimal (*A*) and maximal suppression axes (*B*) and the suppression generated by an annular grating. Data points above and below the unity line in *A* and *B* indicate sub- and super-linear summation, respectively. *C*: the relationship between suppression generated on the minimal and maximal suppression axes. ● and ○, P and M cells, respectively.

the locations of suppressive areas relative to the receptive field and their absolute positions within the visual field across our sample of cells. Figure 7*A* shows the spatial distribution of suppressive areas when four positions were probed outside the receptive field. Each data point represents the end of an *SI* vector, the angular position of which represents the location of a suppressive area. The circles and squares represent SI_1 and SI_2 vectors, respectively. It is clear that the scatter of data points in each plot does not suggest any systematic organization to suppressive areas outside the receptive field.

It is possible that the spatial asymmetry in suppression we describe here arises as a consequence of the nonuniform distribution of cones in the retina. The rapid decline of cone density with eccentricity and their higher density in nasal retina than in temporal retina (Troilo et al. 1993) could mean that the strength of signals arising from foveal or nasal retina is proportionally stronger than from peripheral or temporal retina, respectively. We examine this possibility in Fig. 7*B*, where we plot the visual field locations of receptive fields receiving spatially asymmetrical suppression. The data points in this plot represent receptive-field locations for each cell, and the lines emanating from them represent their respective SI_I vectors, pointing to the location in the visual field where most suppression arose. The length of each vector is proportional to the magnitude of suppression originating from that location in the visual field. If suppressive signals originating in the fovea were stronger than from the periphery, then most SI_I vectors should point toward the fovea, represented by the origin in this plot. Alternatively, if suppressive signals were stronger from nasal than temporal retina then most SI_I vectors should point away from the vertical meridian. It is clear that the SI_I vectors do not point in a single direction. Indeed, the directions of the SI_I vectors appears randomly distributed, suggesting that asymmetrical suppression outside the receptive fields of LGN cells is not mediated by the relatively higher density of cones in foveal and/or nasal retina.

DISCUSSION

We characterized the spatial distribution of suppression outside the classical receptive field in LGN. For a subset of cells in our sample, there was clear deviation from circular symmetry in the suppressive surround. For these cells, suppressive signals were spatially asymmetrical or balanced in opposing areas outside the receptive field. A suppressive area was larger than the receptive field itself and summation of suppressive signals was nonlinear. The nonuniform distribution of cones in the retina did not account for the asymmetrical distribution of suppressive signals.

These findings raise two fundamental questions. What is the origin of suppressive signals in the suppressive surround of LGN cells? Is surround suppression in V1 cells inherited from the LGN?

Origin of the suppressive surround in LGN

Unlike the classical receptive field of most LGN cells (Derrington and Lennie 1984; Kremers et al. 2001), the suppressive surround is insensitive to spatiotemporal modulation (Solomon et al. 2002), spatially summates light signals nonlinearly, and is spatially extensive (results reported here). These observations suggest that the classical receptive field and suppressive surround are constructed by different mechanisms and are likely to have different origins. We have considered and rejected one potential source of the suppressive signal—the nonuniform distribution of cones in the retina (Troilo et al. 1993). The spatial asymmetry of suppression outside the receptive field of LGN cells does not match the asymmetry of cones in foveal and nasal retina. However, this does not rule out nonuniform retinal wiring as a potential source of suppressive signals. They may have their origin in the inhibitory amacrine and horizontal cell network, although this pathway is likely to be different from that which constructs the classical surround (McMahon et al. 2004).

Local inhibitory projections from the thalamic reticular nucleus or within the LGN are also potential sources of the suppressive signal. Inhibitory input from thalamic reticular cells mediates at least one form of long-range suppression in LGN (Funke and Eysel 1998). However, the stimulation regime used in that study was quite distinct from that used here and similar to that used to study the "shift-effect" in retinal and LGN cells (Barlow et al. 1977; Felisberti and Derrington 2001a,b; Kruger and Fischer 1973; McIlwain 1964, 1966), which probably has different properties to (nonclassical) surround suppression (Solomon et al. 2002). The receptive-field properties and pattern of connections of interneurons within the LGN seem more suited to mediate surround suppression. In cats, receptive fields of geniculate interneurons have a similar center-surround organization to relay cells (Dubin and Cleland 1977; Mastronarde 1992), and each relay cell receives inhibitory input from several interneurons with receptive fields spatially offset from the relay cell itself (Singer and Creutzfeldt 1970). If interneuron receptive fields are organized this way in primates, then this pattern of inhibitory input is a likely source of the spatially nonuniform suppression we describe here. The attractiveness of this prediction is that different spatial configurations of interneuron receptive fields could give rise to different spatial patterns of suppression outside the receptive fields of relay cells.

Surround suppression in LGN and visual cortex

Despite an intensive examination of surround suppression in visual cortical cells in recent years, we have yet to identify the origin of the suppressive signal. A recent study in cats (Ozeki et al. 2004) challenged the widely held view that surround suppression is mediated by intra-cortical inhibition (Angelucci et al. 2002a,b; Bair et al. 2003; Bullier et al. 2001; Cavanaugh et al. 2002a; DeAngelis et al. 1994; Walker et al. 1999, 2002). Ozeki et al. concluded that surround suppression in visual cortex originates from reduced excitatory input from LGN neurons. The spatial pattern of surround suppression in LGN and V1 are very different, however, suggesting that the suppressive surround in V1 is not simply inherited from LGN. In cat V1, the suppressive surround is orientation tuned and has similar spatial dimensions to the classical receptive field (Walker et al. 1999), whereas in marmoset LGN it is not orientation tuned (Solomon et al. 2002) and is considerably larger than an LGN or V1 receptive field (results reported here). Walker and colleagues also examined the spatial distribution of suppression in a small sample of cat LGN cells. Careful examination of their example cell in which suppression

arose asymmetrically (see their Fig. 13) suggests that it has similar spatial profile to the cells described here (see Fig. 3, *B* and *D*). This suggests that, as reported here in marmosets, in cat LGN suppression arises from a relatively large area outside the receptive field.

We suggest that the suppressive surrounds of V1 neurons—localized and tuned for orientation—are quite different from those in LGN—large and not tuned. Nevertheless, surround suppression in both areas may perform similar functional roles, reducing redundancy in neural representations of visual scenes (Müller et al. 2003; Schwartz and Simoncelli 2001). In LGN, the broad spatial and temporal tuning requires a broadly tuned surround; in V1, receptive fields are larger and are narrowly tuned—redundancy in these neurons is found in the domain of position and orientation. The advantage of a large, broadly tuned anisotropic suppressive surround in LGN is that redundancy in global contrast signals can be pooled over a wide range of spatial and temporal scales in particular areas of the visual field. A localized, narrowly tuned, anisotropic suppressive surround in V1 may facilitate redundancy reduction of local, oriented contrast signals. A challenge ahead is to establish whether surround suppression is a purpose-built redundancy reduction mechanism that contributes to efficient neural coding along early visual pathways or is simply an accidental consequence of neural wiring.

ACKNOWLEDGMENTS

We thank P. Lennie for allowing us to use his software, S. Solomon and J. Peirce for comments on the manuscript, and N. Barraclough for helping with some of the data collection.

Present address of A. Derrington, C. Tinsley, and C. Vincent: Henry Wellcome Bldg., University of Newcastle on Tyne, Newcastle on Tyne, UK.

GRANTS

This work was supported by a Wellcome Trust prize studentship to B. S. Webb and Wellcome Trust program grant to A. M. Derrington.

REFERENCES

Allman J, Miezin F, and McGuinness E. Stimulus specific responses from beyond the classical receptive field: neurophysiological mechanisms for local-global comparisons in visual neurons. *Annu Rev Neurosci* 8: 407–430, 1985.

Angelucci A, Levitt JB, and Lund JS. Anatomical origins of the classical receptive field and modulatory surround field of single neurons in macaque visual cortical area V1. *Prog Brain Res* 136: 373–388, 2002a.

Angelucci A, Levitt JB, Walton EJS, Hupé JM, Bullier J, and Lund JS. Circuits for local and global signal integration in primary visual cortex. *J Neurosci* 22: 8633–8646, 2002b.

Bair W, Cavanaugh JR, and Movshon JA. Time course and time-distance relationships for surround suppression in macaque V1 neurons. *J Neurosci* 23: 7690–7701, 2003.

Barlow HB, Derrington AM, Harris LR, and Lennie P. The effects of remote retinal stimulation on the responses of cat retinal ganglion cells. *J Physiol* 269: 177–194, 1977.

Batschelet E. *Circular Statistics in Biology.* New York: Academic, 1981.

Bullier J, Hupé JM, James AC, and Girard P. The role of feedback connections in shaping the responses of visual cortical neurons. *Prog Brain Res* 134: 193–204, 2001.

Cavanaugh JR, Bair W, and Movshon JA. Nature and interaction of signals from the receptive field center and surround in macaque V1 neurons. *J Neurophysiol* 88: 2530–2546, 2002a.

Cavanaugh JR, Bair W, and Movshon JA. Selectivity and spatial distribution of signals from the receptive field surround in macaque V1 neurons. *J Neurophyiols* 88: 2547–2556, 2002b.

Cleland BG, Lee BB, and Vidyasagar TR. Responses of neurons in the cat's lateral geniculate nucleus to moving bars of different length. *J Neurosci* 3: 108–116, 1983.

Cudeiro J and Sillito AM. Spatial frequency tuning of orientation-discontinuity-sensitive corticofugal feedback to the cat lateral geniculate nucleus. *J Physiol* 490: 481–492, 1996.

DeAngelis GC, Freeman RD, and Ohzawa I. Length and width tuning of neurons in the cat's primary visual cortex. *J Neurophysiol* 71: 347–374, 1994.

Derrington A and Lennie P. Spatial and temporal contrast sensitivities of neurones in lateral geniculate nucleus of macaque. *J Physiol* 357: 219–240, 1984.

Dubin MW and Cleland BG. Organization of visual inputs to interneurons of the lateral geniculate nuceus of the cat. *J Neurophysiol* 40: 410–428, 1977.

Felisberti F and Derrington AM. Long-range interactions in the lateral geniculate nucleus of the New-World monkey, *Callithrix jacchus. Vis Neurosci* 18: 209–218, 2001a.

Felisberti F and Derrington AM. Long-range interactions modulate the contrast gain in the lateral geniculate nucleus of cats. *Vis Neurosci* 16: 943–956, 2001b.

Funke K and Eysel UT. Inverse correlation of firing patterns of single topographically matched perigeniculate neurons and cat dorsal lateral geniculate relay cells. *Vis Neurosci* 15: 711–729, 1998.

Hubel DH and Wiesel TN. Integrative action in the cat's lateral geniculate body. *J Physiol* 155: 385–398, 1961.

Jones HE, Andolina IM, Oakely NM, Murphy PC, and Sillito AM. Spatial summation in lateral geniculate nucleus and visual cortex. *Exp Brain Res*: 279–284, 2000.

Jones HE, Grieve KL, Wang W, and Sillito AM. Surround suppression in primate V1. *J Neurophysiol* 86: 2011–2028, 2001.

Jones HE and Sillito AM. The length-response properties of cells in the feline dorsal lateral geniculate nucleus. *J Physiol* 444: 329–448, 1991.

Kremers J, Carlos L, Silveira L, and Kilavik B. Influence of contrast on the responses of marmoset lateral geniculate cells to drifting gratings. *J Neurophysiol* 85: 235–246, 2001.

Kruger J and Fischer B. Strong periphery effect in cat retinal ganglion cells. Excitatory responses in ON and Off center neurons to single grid displacements. *Exp Brain Res* 18: 316–318, 1973.

Levick WR, Cleland BG, and Dubin MW. Lateral geniculate neurons of cat: retinal inputs and physiology. *Invest Opthalmol Vis Sci* 11: 302–311, 2002.

Marrocco RT and McClurkin JW. Evidence for spatial structure in the cortical input to the monkey lateral geniculate nucleus. *Exp Brain Res* 59: 50–56, 1985.

Marrocco RT, McClurkin JW, and Young RA. Modulation of lateral geniculate nucleus cell responsiveness by visual activation of the corticogeniculate pathway. *J Neurosci* 1982: 256–263, 1982.

Mastronarde DN. Nonlagged relay cells and interneurons in the cat lateral geniculate nucleus: receptive-field properties and retinal inputs. *Vis Neurosci* 8: 407–441, 1992.

McClurkin JW and Marrocco RT. Visual cortical input alters spatial tuning in monkey lateral geniculate nucleus cells. *J Physiol* 348: 135–152, 1984.

McIlwain JT. Receptive fields of optic tract axons and lateral geniculate cells: peripheral extent and barbiturate sensitivity. *J Neurophysiol* 27: 1154–1173, 1964.

Mcllwain JT. Some evidence concerning the physiological basis of the periphery effect in the cat's retina. *Exp Brain Res* 1: 265–271, 1966.

McMahon MJ, Packer OS, and Dacey DM. The classical receptive field surround of primate parasol ganglion cells is mediated primarily by a non-GABAergic pathway. *J Neurosci* 24: 3736–3745, 2004.

Molotchnikoff S and Cérat A. Responses from outside classical receptive fields of dorsal lateral geniculate cells in rabbits. *Exp Brain Res* 92: 94–104, 1992.

Müller JR, Metha AB, Krauskopf J, and Lennie P. Local signals from beyond the receptive fields of striate cortical neurons. *J Neurophysiol* 90: 822–831, 2003.

Murphy PC and Sillito AM. Corticofugal feedback influences the generation of length tuning in the visual pathway. *Nature* 329: 727–729, 1987.

Ozeki H, Sadakane O, Akasaki T, Naito T, Shimegi S, and Sato H. Relationship between excitation and inhibition underlying size tuning and contextual response modulation in the cat primary visual cortex. *J Neurosci* 24: 1428–1438, 2004.

Rivadulla C, Martínez L, Varela C, and Cudeiro J. Completing the corticofugal loop: a visual role for the cortocogeniculate type 1 metabotropic glutamate receptor. *J Neurosci* 22: 2956–2962, 2002.

Schwartz O and Simoncelli EP. Natural signal statistics and sensory gain control. *Nature Neurosci* 4: 819–825, 2001.

Sillito AM, Cudeiro J, and Murphy P. Orientation sensitive elements in the corticofugal influence on center-surround interactions in the dorsal lateral geniculate nculeus. *Exp Brain Res* 93: 6–16, 1993.

Singer W and Creutzfeldt OD. Reciprocal lateral inhibition of on- and off-centre neurones in the lateral geniculate body of the cat. *Exp Brain Res* 10: 311–330, 1970.

Solomon SG, White JR, and Martin PR. Extraclassical receptive field properties of parvocellular, magnocellular and koniocellular cells in the primate lateral geniculate nucleus. *J Neurosci* 22: 338–349, 2002.

Troilo D, Howland H, and Judge S. Visual optics and retinal cone topography in the common marmoset (*Callithrix jacchus*). *Vis Res* 33: 1301–1310, 1993.

Vidyasagar TR and Urbas JV. Orientation sensitivity of cat LGN neurones with and without inputs from visual cortical areas 17 and 18. *Exp Brain Res* 46: 157–169, 1982.

Walker GA, Ohzawa I, and Freeman RD. Asymmetric suppression outside the classical receptive field of the visual cortex. *J Neurosci* 19: 10536–10553, 1999.

Walker GA, Ohzawa I, and Freeman RD. Disinhibition outside receptive fields in the visual cortex. *J Neurosci* 22: 5659–5668, 2002.

Webb BS, Tinsley CJ, Barraclough NE, Easton A, Parker A, and Derrington AM. Feedback from V1 and inhibition from beyond the classical receptive field modulates the responses of neurons in the primate lateral geniculate nucleus. *Vis Neurosci* 19: 583–592, 2002.

Webb BS, Tinsley CJ, Barraclough NE, Parker A, and Derrington AM. Gain control from beyond the classical receptive field in primate primary visual cortex. *Vis Neurosci* 20: 221–230, 2003.

Xiao DK, Raiguel S, Marcar V, Koenderink J, and Orban GA. Spatial heterogeneity of inhibitory surrounds in the middle temporal visual area. *Proc Natl Acad Sci USA* 92: 11303–11306, 1995.